

Coordination Modes in a Tridentate NNS (Thiosemicarbazonato)copper(II) System Containing Oxygen-Donor Coligands – Structures of $[\{\text{Cu}(\text{L})(\text{X})\}_2]$ ($\text{X} = \text{Formato, Propionato, Nitrito}$)

Patricia Gómez-Saiz,^[a] Javier García-Tojal,^{*[a]} Aránzazu Mendiá,^[a] Bruno Donnadiéu,^[b] Luis Lezama,^[c] José Luis Pizarro,^[d] Maria Isabel Arriortua,^[d] and Teófilo Rojo^[c]

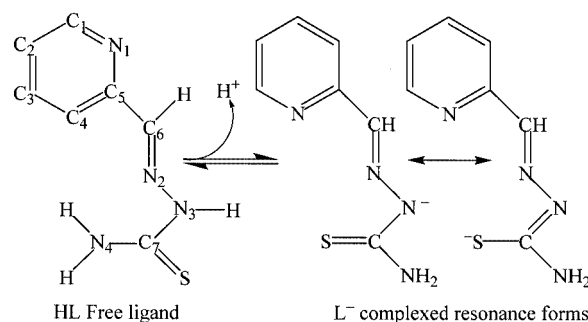
Keywords: Copper / Magnetic properties / Stacking interactions / Thiosemicarbazone complexes

Complexes with the formula $[\{\text{Cu}(\text{L})\text{X}\}_2]$ [$\text{X} = \text{HCOO}^-$ (**1**), $\text{CH}_3\text{CH}_2\text{COO}^-$ (**2**), NO_2^- (**3**)], where $\text{HL} = \text{C}_7\text{H}_8\text{N}_4\text{S}$ (pyridine-2-carbaldehyde thiosemicarbazone), have been synthesised and characterised. Single-crystal X-ray diffraction studies show that the structures of these compounds consist of centrosymmetric dimers containing distorted square-pyramidal copper(II) ions. The metal centres are coordinated to the NNS atoms of the tridentate thiosemicarbazonato ligand and one oxygen atom of the X coligand in the basal position. These complexes mainly differ in the atom that occupies the apical position. The structures of compounds **1** and **3** are made up of $[\text{Cu}_2(\mu\text{-SL})_2]$ entities in which the sulfur atom of the tridentate ligand acts as a bridge occupying the apical

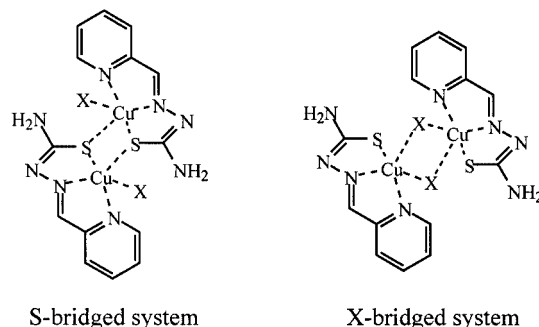
position. Compound **2** contains a $[\text{Cu}_2(\mu\text{-OX})_2]$ species bridged through the oxygen atoms from both propionato ligands. The results demonstrate the influence of the size of the coligand on the structure of these complexes. Structural and spectroscopic results suggest the presence of relevant ligand-to-metal charge transfers in these compounds. The EPR spectra exhibit rhombic symmetry. Magnetic measurements show antiferromagnetic couplings. The susceptibility data were fitted using the Bleaney–Bowers equation for copper(II) dimers. The J/k values obtained are -4.0 , -4.8 and -4.9 K for compounds **1**, **2** and **3**, respectively. (© Wiley-VCH Verlag GmbH & Co. KGaA, 69451 Weinheim, Germany, 2003)

Introduction

In the last 30 years, thiosemicarbazones and their metal complexes have been extensively studied due to their relevant biological properties.^[1] In particular, the copper(II) derivatives of pyridine-2-carbaldehyde thiosemicarbazone ($\text{HL} = \text{C}_7\text{H}_8\text{N}_4\text{S}$) have drawn much attention (see Scheme 1). This thiosemicarbazone ligand coordinates to the metal ions in both the anionic (L^-) and neutral (HL) forms. The anionic L^- form is usually present in $[\{\text{Cu}(\text{L})\text{X}\}_2]$ dimers. In these dinuclear compounds, the metal centres can either be bridged through the sulfur enethiolato atom ($\text{X} = \text{Cl, Br, NCS}$)^[2,3] or the non-thiosemicarbazone coligands^[4,5] ($\text{X} = \text{CH}_3\text{CH}_2\text{COO}^-$, Scheme 2). In recent work, we have tried to rationalise the structural,



Scheme 1



Scheme 2

^[a] Departamento de Química, Universidad de Burgos
Plaza Misael Bañuelos s/n, 09001 Burgos, Spain
Fax: (internat.) + 34-947/258831
E-mail: qipgatoj@ubu.es

^[b] Laboratoire de Chimie de Coordination du CNRS
205 route de Narbonne, 31077 Toulouse Cedex, France

^[c] Departamento de Química Inorgánica, Universidad del País Vasco
Aptdo. 644, 48080 Bilbao, Spain

^[d] Departamento de Mineralogía-Petrología, Universidad del País Vasco
Aptdo. 644, 48080 Bilbao, Spain

spectroscopic and magnetic aspects of this system by means of comparative structural studies and approximate molecular orbital calculations.^[6] Several structural differences between dinuclear S- and X-bridged complexes have been found. The presence of S-bridges is due to $p + sp^2$ hybridising of the thiolato sulfur atom. The results suggest that the electron density of the S p_z orbital in the S-bridged systems is less delocalised towards the thiosemicarbazone chain than that of the X-bridged complexes. The formation of complexes with the S-bridge as opposed to the X-bridge depends on the nature of the non-thiosemicarbazone ligands. However, the actual underlying reasons for the formation of S- over X-bridged systems are not clear to date.

In order to evaluate the influence of the size and the type of O-donor coligand in the structure of these compounds, we present the synthesis, crystal structure, spectroscopic and magnetic properties of the $[Cu(L)X]_2$ [$X = HCOO^-$ (**1**), $CH_3CH_2COO^-$ (**2**), NO_2^- (**3**)] complexes. Approximate molecular orbital calculations of the extended Hückel type have been carried out in order to understand the magnetic features of these systems.

Results and Discussion

The pyridine-2-carbaldehyde thiosemicarbazone (HL) ligand and the $[Cu(L)(NO_3)]$ complex used as starting materials were synthesised according to published methods with slight modifications.^[7,8] Elemental analyses are consistent with the proposed stoichiometries. Crystallographic details are given in Table 1.

Discrete quasi-planar $[Cu(L)(HCOO)]$ and $[Cu(L)(NO_2)]$ entities form the crystal structures of compounds **1** and **3**, respectively, linked through the sulfur atom of the thiosemicarbazonato ligand, which leads to dinuclear centrosymmetric $[Cu(L)X]_2$ species. The molecular structures are shown in Figures 1 and 2. Selected interatomic dimensions are given in Table 2. The copper(II) ions are five-coordinate with two nitrogen atoms and one sulfur atom from the thiosemicarbazonato ligand [Cu–N(1), N(2), S: 2.016(4), 1.976(4), 2.265(2), and 2.025(3), 1.974(3), 2.268(1) Å for **1** and **3**, respectively] and an oxygen atom from one of the formate/nitrito ligands [Cu–O(1) 1.956(4) and 1.964(3) Å] in the basal position. The axial position is occupied by the sulfur atom belonging to the thiosemicarbazonato ligand of

Table 1. Summary of crystallographic data and parameters for **1**, **2** and **3**

	1	2	3
Empirical formula	$C_{16}H_{16}Cu_2N_8O_4S_2$	$C_{20}H_{24}Cu_2N_8O_4S_2$	$C_{14}H_{14}Cu_2N_{10}O_4S_2$
Formula mass	575.56	631.68	577.56
Crystal size [mm]	$0.30 \times 0.20 \times 0.07$	$0.15 \times 0.10 \times 0.07$	$0.14 \times 0.10 \times 0.04$
System	triclinic	triclinic	triclinic
Space group	$P\bar{1}$	$P\bar{1}$	$P\bar{1}$
a [Å]	7.786(2)	8.687(2)	7.734(1)
b [Å]	8.540(2)	8.723(2)	8.776(1)
c [Å]	8.887(2)	9.273(2)	8.836(1)
α [°]	111.64(3)	108.11(3)	68.23(1)
β [°]	98.78(3)	114.28(3)	95.12(1)
γ [°]	109.75(3)	90.27(3)	68.97(1)
V [Å ³]	496.7(2)	601.6(2)	502.4(1)
Z	1	1	1
$F(000)$	580	644	580
$\rho_{\text{calcd.}}$ [g·cm ^{−3}]	1.924	1.743	1.909
μ (Mo- K_α) [mm ^{−1}]	2.397	1.987	2.372
T [K]	160(2)	160(2)	298(2)
λ (Mo- K_α) [Å]	0.71073	0.71073	0.71073
Scan type	ϕ	ω	$\omega/2\theta$
2θ range [°]	3.3–52.1	5.5–52.06	2–25
No. measured reflections	3681	5857	1896
Interval h, k, l	$\pm 8, \pm 9, \pm 9$	$\pm 10, \pm 10, \pm 11$	$\pm 9, -9 \leq k \leq 10, 0 \leq l \leq 10$
Unique reflections	1348	2175	1771
$R(\text{int})$	0.0498	0.0364	0.0326
Refinement method	Full-matrix least squares on F^2		
Data/restraints/parameters	1348/1/158	2175/0/172	1771/0/146
S	1.030	1.182	1.012
w	$1/[\sigma^2(F_o)^2 + (0.0765P)^2]$	$1/[\sigma^2(F_o)^2 + (0.0328P)^2 + 0.864]$	$1/[\sigma^2(F_o)^2 + (0.0283P)^2]$
$R1$ [$I \geq 2\sigma(I)$]	0.0402	0.0317	0.0336
$wR2$ [$I \geq 2\sigma(I)$]	0.1008	0.0830	0.0644
$R1$ (all data)	0.0537	0.0364	0.0912
$wR2$ (all data)	0.1089	0.045	0.0753
Largest diff. peak/hole [e Å ^{−3}]	0.484, −0.726	0.389, −0.463	0.346, −0.362

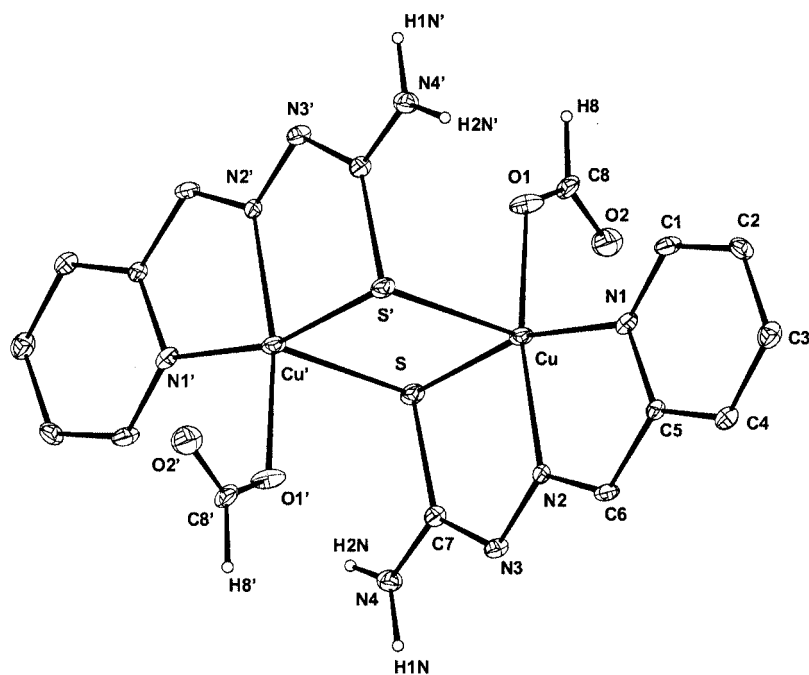


Figure 1. Molecular structure of **1** with thermal ellipsoids at 50% probability level

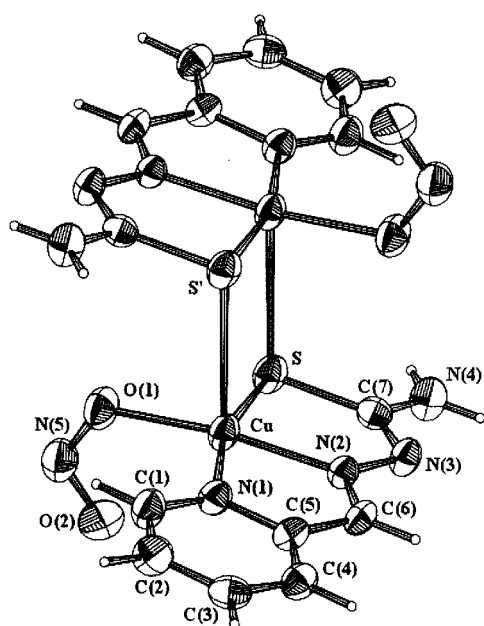


Figure 2. Molecular structure of **3** with thermal ellipsoids at 50% probability level

the adjacent $[\text{Cu}(\text{L})(\text{X})]$ entity [$\text{Cu}-\text{S}'$ 2.820(2) and 2.918(2) Å for **1** and **3**, respectively]. The intramolecular $\text{Cu}\cdots\text{Cu}'$ distance is 3.503(2) Å in **1** and 3.554(1) Å in **3**. The distortion of the coordination polyhedra from square-pyramidal (SP, $\tau = 0$) and trigonal-bipyramidal (TBP, $\tau = 1$) topologies have been analysed.^[9] The τ values obtained were 0.06 (**1**) and 0.13 (**3**), which clearly indicates that the environment of the copper(II) ions is close to the SP topology.

The thiosemicarbazonato ligand exhibits high planarity. The dihedral angles formed by the least-squares planes of both the thiosemicarbazone molecules, inside the dimer, are about 2.4 and 1.5° for **1** and **3**, respectively.

The crystal structure of complex **2** consists of centrosymmetric $[\{\text{Cu}(\text{L})(\text{CH}_3\text{CH}_2\text{COO})\}_2]$ entities. A perspective view of the molecular structure is shown in Figure 3. Several distances and angles are shown in Table 2. Each copper(II) ion exhibits a five-coordinate geometry. It is coordinated by two nitrogen atoms and one sulfur atom of the thiosemicarbazonato ligand [$\text{Cu}-\text{N}(1)$, $\text{N}(2)$, S : 2.056(2), 1.966(2), 2.287(1) Å] and the oxygen O(1) atom of the propionate ligand at 1.951(2) Å, in the basal plane. The oxygen atom belonging to the thiosemicarbazonato ligand of the adjacent $[\text{Cu}(\text{L})(\text{CH}_3\text{CH}_2\text{COO})]$ entity [$\text{Cu}-\text{O}(1')$ 2.387(2) Å] occupies the axial position. The intramolecular $\text{Cu}\cdots\text{Cu}'$ distance is 3.460(2) Å. The distortion of the coordination polyhedron gives a value of $\tau = 0.19$ characteristic of a geometry close to that of SP.

The thiosemicarbazonato ligand is nearly planar in complex **2**. Both thiosemicarbazone molecules in the dimer are coplanar (dihedral angle about 0.0°).

As can be expected, the longest C–O/N–O bonds inside the coligands involve the O(1) atoms that are linked to the metal ions, for all three of the complexes.

Several hydrogen bonds are established in the lattice of these compounds in which the O(2), N(3) and N(4) atoms are involved (see Table 2). The presence of C–H \cdots S linkages is also remarkable.

It is worth mentioning that the shortest distances between the pyridine plane and the thiosemicarbazone moiety of different molecules are 3.28 [$\text{C}(3)\cdots\text{C}(7)^{\text{iv}}$], 3.31 [$\text{C}(5)\cdots\text{N}(2)^{\text{iii}}$] and 3.37 Å [$\text{C}(3)\cdots\text{C}(7)^{\text{v}}$] for **1**, **2** and **3**, re-

Table 2. Selected bond lengths [Å] and angles [°] for **1**, **2** and **3**

	1	2	3
Cu–S	2.265(2)	2.287(1)	2.268(1)
Cu–N(1)	2.016(4)	2.056(2)	2.025(3)
Cu–N(2)	1.976(4)	1.966(2)	1.974(3)
Cu–O(1)	1.956(4)	1.951(2)	1.964(3)
Cu–S' / –O(1)'	2.820(2) ⁱ	2.387(2) ⁱⁱ	2.918(2) ⁱⁱⁱ
S–C(7)	1.752(5)	1.735(3)	1.739(4)
N(2)–C(6)	1.271(7)	1.290(4)	1.285(5)
N(2)–N(3)	1.367(6)	1.367(3)	1.365(4)
N(3)–C(7)	1.317(7)	1.330(4)	1.324(5)
N(4)–C(7)	1.329(7)	1.335(4)	1.333(5)
N(2)–Cu–O(1)	167.8(2)	173.98(9)	172.2(1)
S–Cu–N(1)	164.3(1)	162.59(8)	164.40(9)
Cu–X–Cu'	86.34(5)	105.35(9)	85.5(1)
Selected coligand bonds			
O(1)–C(8)/O(1)–N(5)	1.238(7)	1.283(4)	1.279(4)
O(2)–C(8)/O(2)–N(5)	1.220(6)	1.231(4)	1.209(4)
Closest Cu...Cu distances			
Intramolecular	3.503(2) ⁱ	3.460(2) ⁱⁱ	3.554(1) ⁱⁱⁱ
Intermolecular	5.437(2) ^{iv}	5.514(2) ⁱⁱⁱ	5.573(1) ^v
Hydrogen bonding contacts A–H...B			
	A–H [Å]	A...B [Å]	H...B [Å]
1:			
N(4)–H(1n)...N(3) ⁱⁱⁱ	0.94(5)	3.203(6)	2.30(6)
N(4)–H(2n)...O(2) ^{vi}	0.94(5)	3.023(6)	2.15(5)
C(4)–H(4)...S ^{vii}	0.93	3.487(5)	2.820(2)
2:			
N(4)–H(1n)...N(3) ^v	0.88(5)	3.005(5)	2.12(5)
N(4)–H(2n)...O(2) ^{viii}	0.73(6)	3.062(5)	2.56(5)
C(1)–H(1)...S ^{ix}	0.95	3.452(4)	2.879(1)
3:			
N(4)–H(41)...N(3) ^x	0.860(3)	3.167(4)	2.320(3)
N(4)–H(42)...O(2) ^{ix}	0.860(4)	3.298(5)	2.550(3)
C(4)–H(4)...S ^{xi}	0.930(3)	3.514(4)	2.807(1)
ⁱ = –x, –y + 1, –z + 1 ⁱⁱ = –x + 1, –y, –z ⁱⁱⁱ = –x, –y, –z ^{iv} = –x, –y, –z + 1 ^v = –x, –y + 1, –z ^{vi} = –x + 1, –y + 1, –z + 1 ^{vii} = –x + 1, y – 1, z ^{viii} = x, y + 1, z ^{ix} = –x + 1, –y, –z ^x = –x, –y + 1, –z – 1 ^{xi} = x – 1, y + 1, –z ⁱⁱ = –x – 1, –y + 1, –z			

spectively. This suggests the existence of π – π stacking of the slipped packing type^[10] as represented in Figure 4. These interactions have been evaluated,^[11,12] and the results are shown in Table 3. The coordination of a metal ion to the nitrogen heteroatom of pyridines and other heterocycles enhances the electron-withdrawing effect through its positive charge, and hence the stability of the π – π interaction increases.^[13,14] These kinds of interactions have been observed in other thiosemicarbazone systems.^[15–18]

Complexation induces conformational changes in the ligand. Atoms N(1) and N(2) are *anti* with respect to the C(5)–C(6) bond in the free ligand;^[19] however, they become *syn* after chelation. Furthermore, the N(2) and S atoms are *anti* with respect to the N(3)–C(7) bond in the free ligand^[19] and also in the pyridinium (H₂L)Cl·H₂O

cationic derivative,^[20] but they are *syn* in the metal complexes. The C–C and C–N distances are similar to those found in the free ligand and its cationic form, except for the N(3)–C(7) and C(7)–S bond lengths, which are 1.358(4) and 1.698(3) Å, respectively, in the free ligand. This suggests that the double bond character of the N(3)–C(7) and C(7)–S bonds increases and decreases, respectively, in the complexed thiosemicarbazonato ligand. However, bond lengths are often in the range of the experimental error and other structural parameters such as some of the bond angles and non-contact distances are more appropriate to evaluate the anionic vs. neutral character of the ligand upon complexation.^[6] The results summarised in Table 4 show that the distances and angles for the title complexes are in good agreement with those expected for compounds con-

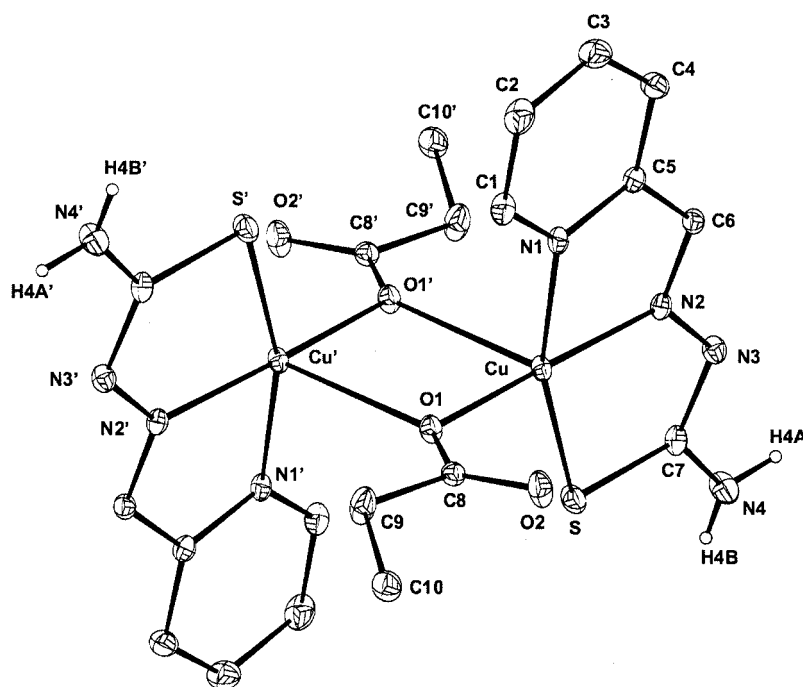


Figure 3. Molecular structure of **2** with thermal ellipsoids at 50% probability level

taining the pyridine-2-carbaldehyde thiosemicarbazone ligand in the anionic form.

The presence of μ -thiolato bridges between the metal centres in the iminothiolato systems such as heterocyclic thiosemicarbazone complexes is unusual,^[21] although they have been found in other related thiosemicarbazone compounds.^[2,3,17,22–28]

The existence of different infrared absorptions corresponding to the thioamide and pyridine substituents, together with the electron delocalisation through the thiosemicarbazone molecule, make the assignation of the bands in these compounds difficult. The intense bands around 1600 cm^{-1} can be attributed to the $\nu(\text{C}=\text{N})_{\text{azomethine}}$, $\nu(\text{C}=\text{N})_{\text{pyridine}}$ and $\delta(\text{NH}_2)$ modes. The strong band at 1525 cm^{-1} in the free ligand has been identified as corresponding to a thioamide I absorption, with high contribution of the $\delta(\text{NH}_2)$ and $\delta(\text{NH})$ deformation modes. This band undergoes an increase in energy on complexation^[29] and its intensity decreases in the compounds containing the deprotonated ligand. The thioamide IV band, which appears at 820 cm^{-1} in the free ligand, is absent in the copper(II) complexes. This is probably due to both a decrease in the double bond character of the C7–S bond and the change in the conformation of the N3–C7 bond on complexation.^[3] Other absorptions observed in the $815\text{--}830\text{ cm}^{-1}$ region for **2** and **3** have been attributed to the coligand (see below). The bands at ca. 447 cm^{-1} have been assigned to the $\nu(\text{Cu}-\text{N}_{\text{azomethine}})$ vibration. These results indicate the presence of the thiosemicarbazonato ligand coordinated to the copper(II) ions through the $\text{N}_{\text{pyridine}}\text{N}_{\text{azomethine}}\text{S}$ chelating centres.

The very strong bands at 1616 and 1316 cm^{-1} in **1** have been attributed to the $\nu(\text{C}=\text{O})$ and $\nu(\text{C}-\text{O})$ absorptions of

the formate ligand [the latter overlapped with a thioamide III absorption mainly due to $\delta(\text{N}-\text{H})$ and $\nu(\text{C}-\text{N})$ contributions of the thiosemicarbazone]. The Δ value [$\nu_a(\text{COO}) - \nu_s(\text{COO})$ in the free ion] is 300 cm^{-1} for **1**, which is greater than the value of 201 cm^{-1} observed for the ionic formate, in good agreement with the unidentate character of the coligand.^[30] Unfortunately, the complexity of the spectrum of compound **2** only allows for the distinction of the strong band at 1603 cm^{-1} , due to the overlapped $\nu(\text{C}=\text{O})$ and thioamide I absorptions [$\delta(\text{N}-\text{H})$ and $\nu(\text{C}=\text{N})$ contributions]. A weak band at 816 cm^{-1} appears in the infrared spectrum of **2** which is also present for the sodium propionate, and can be attributed to $\nu(\text{C}-\text{C})$ vibration modes of the propionato ligand.

The infrared spectrum of compound **3** shows a shoulder at around 1408 cm^{-1} and two bands at 1125 and 826 cm^{-1} . These bands are attributed to the $\nu(\text{N}=\text{O})$, $\nu(\text{N}-\text{O})$ and $\delta(\text{ONO})$ absorptions of the nitrito ligand.^[31]

The reflectance spectra of the title compounds show bands in the $220\text{--}235$, $260\text{--}270$, $360\text{--}465$ and $590\text{--}750\text{ nm}$ regions. These are assigned to $(\pi \rightarrow \pi^*)_{\text{pyridine}}$, $(n \rightarrow \pi^*)_{\text{pyridine}}$, $(n \rightarrow \pi^*)_{\text{thiosemicarbazone}}$, LMCT N/O/S \rightarrow d and d \rightarrow d transitions, respectively.^[32,33]

The intense absorption observed in the $384\text{--}405\text{ nm}$ range is attributed to a S \rightarrow Cu^{II} charge transfer transition.^[3] The absorptions between $430\text{--}465\text{ nm}$ may be due to LMCT O/N \rightarrow Cu^{II} transitions, as were observed in other related compounds.^[34]

The maxima observed from the solid samples in the $595\text{--}650\text{ nm}$ region are characteristic of d \rightarrow d transitions for compounds exhibiting a square pyramidal geometry with a $d_{x^2-y^2}$ ground state. These bands show unresolved shoulders obscured by the tails above 700 nm , which can be

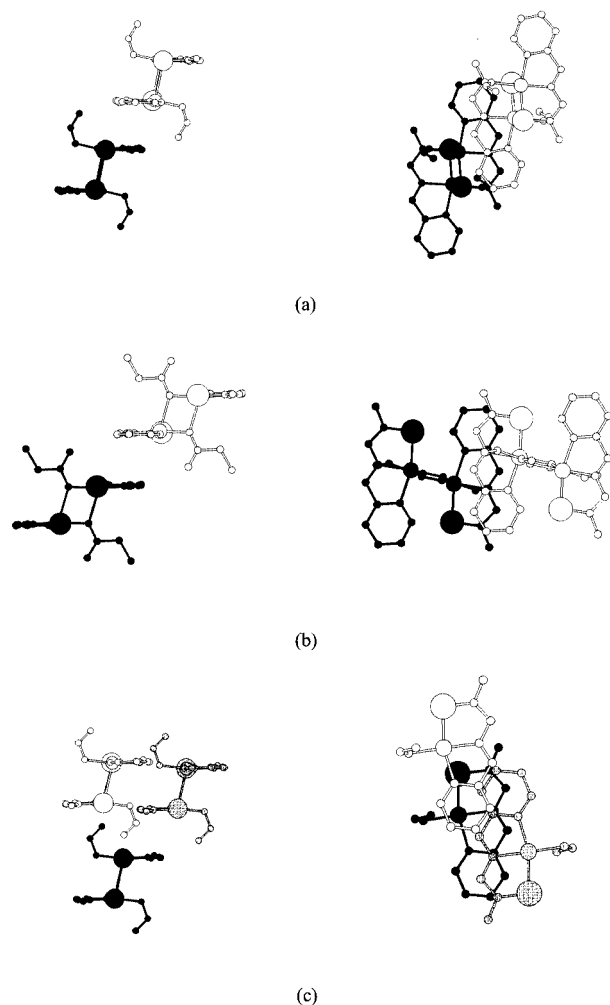


Figure 4. Details of π – π stacking for (a) **1**, (b) **2** and (c) **3**; drawing (c) on the right represents monomeric fragments for a clearer view

Table 3. π – π stacking interactions; the symmetry transformations follow the nomenclature used in Table 2; 1: N(1), C(1), C(2), C(3), C(4), C(5) ring in compound **1**; 2: C(6), N(2), N(3), C(7) set in compound **1**, N(3) is considered as the “centroid”; 3: N(1), C(1), C(2), C(3), C(4), C(5) ring in compound **2**; 4: C(6), N(2), N(3), C(7) set in compound **2**, N(3) is considered as the “centroid”; 5: N(1), C(1), C(2), C(3), C(4), C(5) ring in compound **3**; 6: C(6), N(2), N(3), C(7) set in compound **3**, N(3) is considered as the “centroid”; DC: distance [Å] between the centroids of the sets i and j ; ANG: angle [°] between the least-squares planes; DZ: distance [Å] between the “centroid” of the j plane and the least-squares plane of the i ring; DZ': distance [Å] between the centroid of the i ring and the least-squares plane of j ; DXY: distance [Å] between the “centroids” of i and j projected onto the least-squares plane of i ; DXY': distance [Å] between the “centroids” of i and j projected onto the least-squares plane of j ; DS: distance [Å] from the centroid of j to the nearest hydrogen atom of the i ring

i	j	DC	ANG	DZ	DXY	DZ'	DXY'	DS
1	2 ^{iv}	3.34	1.83	3.31	0.26	3.34	0.18	4.01
3	4 ⁱⁱⁱ	3.29	4.40	3.27	0.06	3.17	0.07	3.99
5	5 ^{xii}	4.10	0.00	3.39	2.26	3.39	2.26	3.52
5	6 ^v	3.42	1.62	3.40	0.37	3.39	0.37	4.04

attributed to a certain amount of distortion of the coordination polyhedra to trigonal bipyramidal, in these compounds.

The three compounds exhibit the same solution spectrum with bands at 280, 317 (sh), 382 and 629 nm (see Exp. Sect.), which is basically the same as that previously described for the acetato^[35,36] and the nitrate derivatives.^[3,5] This shows that the coligand has been removed from the coordination sphere indicating the possible existence of entities of type $[\text{CuL}(\text{H}_2\text{O})_3]^+$ in aqueous solution, in good agreement with the close to 1:1 electrolyte character of these compounds in water.

The X-band EPR spectra of polycrystalline samples of the title complexes are shown in Figure 5. They all exhibit rhombic signals. The g values obtained are given in Table 5. These values are similar to those observed for other pyridine-2-carbaldehyde thiosemicarbazone derivatives containing copper(II) ions in distorted square-pyramidal topologies, with a $d_{x^2-y^2}$ ground state.^[2,3,5,6] The O-bridged dimer is the most rhombic and has the largest value for g_1 , which is in good accordance with the differences in the crystal structure.

The plot of the molar susceptibility (χ_m), together with the $\chi_m T$ vs. T curve for **1** is given in Figure 6. The results are very similar to those of complexes **2** and **3**. In all cases, the magnetic measurements obey the Curie–Weiss law at temperatures higher than 50 K. The Weiss temperatures are -2.72 (**1**), -3.29 (**2**) and -3.02 K (**3**). The C_m experimental value is approximately $0.41 \text{ cm}^3 \cdot \text{K} \cdot \text{mol}^{-1}$ and the calculated μ_{eff} values at room temperature are 1.80 BM for all of the compounds. The χ_m values increase with decreasing temperature, reaching a maximum at 5.0 [$0.040 \text{ cm}^3 \text{ mol}^{-1}$ (**1**)], 6.0 [$0.033 \text{ cm}^3 \text{ mol}^{-1}$ (**2**)] and 5.5 [$0.033 \text{ cm}^3 \text{ mol}^{-1}$ (**3**)] K. The $\chi_m T$ value continuously decreases on lowering the temperature indicating the presence of antiferromagnetic interactions in these compounds.

Taking the dimeric nature of these complexes into account, we fitted the susceptibility data using the expression given by Bleaney–Bowers for copper(II) dinuclear compounds [Equation (1)],^[37] derived from the Heisenberg isotropic spin Hamiltonian ($H = -2J S_1 S_2$), for two coupled $S = 1/2$ ions; where $N\alpha = 60 \times 10^{-6} \text{ cm}^3 \text{ mol}^{-1}$ per copper(II) ion, N = Avogadro number, β = Bohr magneton, and k = Boltzmann constant.

$$\chi = \frac{Ng^2\beta^2}{kT} \left(\frac{2}{3 + \exp(-2J/kT)} \right) + N\alpha \quad (1)$$

The best least-squares fit (solid line in Figure 6) is obtained from the parameters $J/k = -4.0 \text{ K}$ (-2.8 cm^{-1}), -4.8 (-3.3 cm^{-1}) and -4.9 K (-3.4 cm^{-1}). The g values are 2.09, 2.10 and 2.09 for the formato, propionato and nitrito complexes, respectively. These g values are in good agreement with those obtained from EPR spectroscopy, 2.083 (**1**), 2.091 (**2**) and 2.090 (**3**). Taking into account the structural features, the existence of interdimeric magnetic

Table 4. Selected structural differences between copper(II) complexes containing neutral (HL) and anionic (L^-) pyridine-2-carbaldehyde thiosemicarbazone ligand [\AA , $^\circ$]

Compound	N(2)–N(3)–C(7)	S–C(7)–N(3)	S–C(7)–N(4)	Cu...N(3)	N(2)...C(7)
1	111.6(4)	125.2(4)	117.1(4)	2.98	2.22
2	111.6(2)	125.3(2)	119.3(2)	2.96	2.23
3	111.6(3)	125.2(3)	118.3(3)	2.97	2.23
HL range	116–118	121–122	121–123	2.89–2.90	2.28–2.32
L^- range	109–114	123–127	117–119	2.94–3.00	2.22–2.23

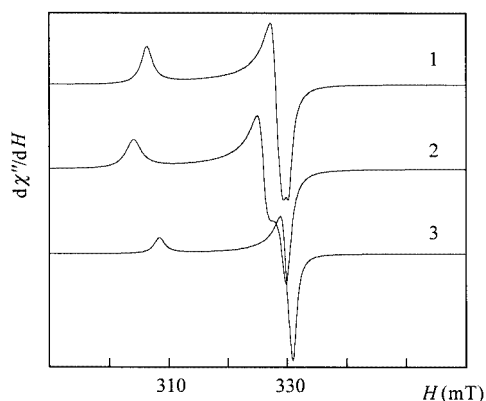
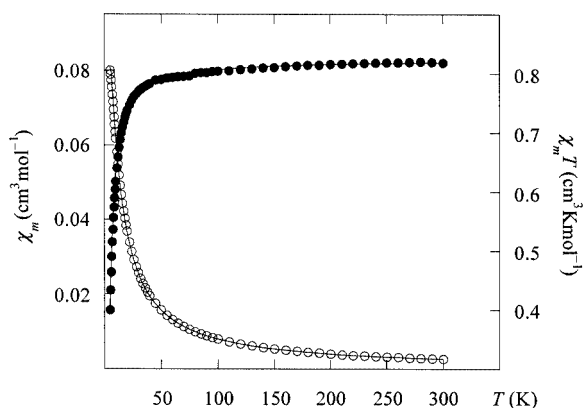
Figure 5. X-band EPR spectra of (a) **1**, (b) **2** and (c) **3** in the solid state at room temp.

Table 5. Experimental EPR spectroscopic parameters

	Temperature	g_1	g_2	g_3
1	room temp. ^[a]	2.183	2.037	2.029
2	room temp. ^[a]	2.198	2.050	2.026
3	room temp. ^[a]	2.186	2.046	2.038

^[a] No variation in the g values from room temperature to 100 K.

Figure 6. Thermal variation of the molar susceptibility (white circles) and $\chi_m T$ (black circles) for **1**; solid lines represent the best fit

interactions should be considered. However, an improvement in the fit was not observed.

The small values of the magnetic interactions suggest that the exchange propagation direction is in a different plane from that formed by the magnetic $d_{x^2-y^2}$ orbitals. These results are in good agreement with the existence of an intradimer exchange coupling in the Cu_2S_2 (**1**, **3**) and Cu_2O_2 (**2**) units.

It has been proposed^[38] that the antiferromagnetic contribution to the magnetic exchange constant J for a dinuclear system with two unpaired electrons is proportional to the square of the energy difference (Δ^2) between the two molecular orbitals constructed from the $d_{x^2-y^2}$ magnetic orbitals. An Extended Hückel molecular orbital (EHMO) analysis has been carried out by means of the CACAO program^[39] to give a qualitative explanation for the magnetic behaviour of these complexes. The EHMO calculations have been carried out using the crystallographic coordinates of the compounds followed by reorientation of the molecules to ensure a maximum overlap.^[40] The data are given in Table 6. The results show a qualitative agreement between Δ^2 and the values of the exchange constant. Unfortunately, the limitations of the EHMO calculations do not allow a perfect sequence to be obtained for very similar J values (for instance, the value of Δ^2 for **3** should be slightly greater than that in **1**, but the opposite trend is observed).

The results obtained of the influence of the bridge angle and the bridge atom are not consistent with those of idealised dimers.^[2,3] One of the factors to be considered is the nature of the terminal coligands placed in the basal plane. In our case, O-donor coligands show the smallest J values. In this sense, it has been established that the less electronegative the donor atom in the basal plane the stronger the induced antiferromagnetic coupling, due to a greater hybridisation of the $d_{x^2-y^2}$ metal orbital towards the bridge.^[41,42] On the other hand, the relationship between J and the bridge angle could be clarified for a given X-donor set. Therefore, it seems that angles close to 90° tend to diminish the J value for compounds containing O-donor basal coligands. This is in good agreement with the results previously reported.^[2] In any case, several concomitant factors could be involved in the values of the exchange coupling constants for these compounds [Cu...Cu intradimer distance, SP vs. BPT distortions around the copper(II) ion, deviation of the metal ion from the basal plane, deviation of the coligand from the basal plane, Cu–X apical distances, etc.]. The synthesis of new (pyridinecarbaldehyde thiosemicarbazono)copper(II) complexes could lead to a better

Table 6. Comparison of the J , Δ^2 and bridging distance and angle values for (pyridine-2-carbaldehyde thiosemicarbazonato)copper(II) dinuclear complexes; the atoms are numbered according to the nomenclature used in the present work (*: average value)

Compound	Bridging atom	Cu–S'/ Cu–X' [Å]	Bridging angle [°]	J [cm ^{−1}]	Δ^2 [eV] ² × 10 ³
[{Cu(NO ₂)(L)} ₂]	S	2.918(2)	85.5(1)	−3.4	1.09
[{CuCl(L)} ₂] ^[2]	S	2.760(2)	87.01(4)	−4.7	11.45
[{CuBr(L)} ₂] ^[2]	S	2.743(2)	87.12(5)	−4.7	17.42
[{Cu(NCS)(L)} ₂] ^[3]	S	2.754(5)*	85.9(1)*	−5.1	45.80
[{Cu(HCOO)(L)} ₂]	S	2.820(2)	86.34(5)	−2.8	1.68
[{Cu(CH ₃ COO)(L)} ₂] ^[26]	O	2.427(2)	103.5(1)	−3.1	1.60
[{Cu(CH ₃ CH ₂ COO)(L)} ₂]	O	2.387(2)	105.35(9)	−3.3	1.85

evaluation of the parameters that influence their magnetic behaviour.

Conclusions

The structural features of these compounds suggest that the increment in the size of the coligand is the main factor that leads to an X- vs. an S-bridge in the [{CuX(L)}₂] systems. These results may serve to rationalise and predict the interactions of the [Cu(L)(H₂O)₃]⁺ entities with biomolecules present in the physiological medium.

Magnetic susceptibility data indicate the presence of weak intradimer antiferromagnetic interactions in these complexes. This behaviour can be qualitatively described from an EHMO study on real molecules.

Experimental Section

Preparation of the Complexes: Thiosemicarbazide, pyridine-2-carbaldehyde, formic and propionic acids, sodium nitrite and copper(II) nitrate were purchased from Probus, Carlo Erba and Fluka. All the complexes were dried under vacuum. The pyridine-2-carbaldehyde thiosemicarbazone (HL) ligand and the [Cu(L)(NO₃)] complex were synthesised according to published methods with slight modifications.^[5,7]

Synthesis of [{Cu(L)(HCOO)}₂] (1): Formic acid (0.23 g, 5 mmol) was slowly added to an aqueous solution of Cu(L)(NO₃) (0.152 g, 0.5 mmol). The pH of the solution was adjusted to 5.5 by the addition of NaOH (1 M). After 1 h, a dark green precipitate was filtered off, washed with water and acetone and dried. The yield was 0.105 g (73%). Crystals suitable for X-ray studies were obtained by diffusion of diethyl ether vapours into a solution of **1** in methanol. C₁₆H₁₆Cu₂N₈O₄S₂ (575.56): calcd. C 33.4, H 2.8, N 19.5, S 11.1; found C 33.3, H 2.8, N 19.4, S 12.0. Molar conductivity of 5·10^{−4} M solutions in water (dimethylformamide) at 25 °C: Λ_M = 102 (4) Ω^{−1} cm² mol^{−1}. Selected IR bands (KBr): $\tilde{\nu}$ = 3290 (m), 3146 (m), 2829 (w), 1634 (s), 1616 (vs), 1602 (vs), 1585 (m, sh), 1559 (w), 1482 (s), 1444 (vs), 1432 (vs), 1381 (s), 1316 (vs), 1264 (m), 1219 (s), 1166 (vs), 1151 (m, sh), 922 (m), 880 (m), 783 (m), 766 (m), 746 (w), 732 (m), 624 (m, b), 449 (w), 416 (m) cm^{−1}. UV/Vis (reflectance spectrum on solid sample): λ_{\max} (ϵ) = ca. 750 (vb, sh), 608 (vb), 463 (b, sh), 405, 267 (sh), 223 nm; (6 × 10^{−5} M water solution): λ_{\max} (ϵ) = 628 (150), 382 (9600), 317 (10600), 280 (14600 M^{−1} cm^{−1}) nm.

Synthesis of [{Cu(L)(CH₃CH₂COO)}₂] (2): This compound was prepared according to an analogous procedure to that of **1** but replacing formic acid with propionic acid (0.37 g, 5 mmol). The bright green product obtained was filtered off, washed with water and acetone and dried. The yield was 0.137 g (87%). Good-quality green crystals were obtained from the mother liquor after some weeks. C₂₀H₂₄Cu₂N₈O₄S₂ (631.68): calcd. C 38.0, H 3.8, N 17.7, S 10.2; found C 37.8, H 3.8, N 17.6, S 9.7. Molar conductivity of 5·10^{−4} M solutions in water (dimethylformamide) at 25 °C: Λ_M = 75 (2) Ω^{−1} cm² mol^{−1}. Selected IR bands (KBr): $\tilde{\nu}$ = 3442 (m), 3290 (m), 3106 (bs), 2974 (m), 1640 (s), 1603 (vs), 1585 (m, sh), 1560 (m), 1485 (m), 1443 (s, sh), 1430 (vs), 1380 (s, b), 1324 (b m), 1271 (s), 1233 (m), 1168 (s), 1153 (s), 931 (w), 880 (m), 816 (w), 764 (w), 738 (m), 630 (m), 449 (w), 415 (w) cm^{−1}. UV/Vis (reflectance spectrum on solid sample): λ_{\max} = 649 (vb), 445 (b, sh), 384, 264, ca. 235 (b, sh) nm.

Synthesis of [{Cu(L)(NO₂)}₂] (3): Sodium nitrite (0.036 g, 0.5 mmol) was allowed to react with an aqueous solution of Cu(L)(NO₃) (0.152 g, 0.5 mmol). Several drops of NaOH (1 M) were added whilst stirring to reach pH ≈ 7. The green precipitate was filtered off, washed with water and acetone and dried. The yield was 0.105 g (73%). Dark green crystals suitable for X-ray studies were separated from the mother liquor by slow concentration at room temperature. C₁₄H₁₄Cu₂N₁₀O₄S₂ (577.56): calcd. C 29.1, H 2.4, N 24.3, S 11.1; found C 28.8, H 2.7, N 23.9, S 10.8. Molar conductivity of 5·10^{−4} M solutions in water (dimethylformamide) at 25 °C: Λ_M = 123 (15) Ω^{−1} cm² mol^{−1}. Selected IR bands (KBr): $\tilde{\nu}$ = 3409 (m), 3280 (m), 3148 (m), 2974 (m), 1627 (s), 1604 (s), 1585 (w), 1560 (w), 1482 (s), 1445 (vs), 1434 (vs), 1408 (s, sh), 1391 (vs), 1320 (m), 1268 (m), 1228 (s), 1169 (vs), 1125 (vs), 914 (s), 878 (m), 826 (w), 775 (s), 743 (s, b), 732 (m, b), 626 (s), 447 (m), 415 (s) cm^{−1}. UV/Vis (reflectance spectrum on solid sample): λ_{\max} = ca. 750 (vb, sh), 593 (vb), 463, 430 (sh), 396 (b), 269, 222 nm.

Physical Measurements: Microanalyses were performed with a LECO CHNS-932 analyser. Conductivity measurements were made with a CRISON 522 conductimeter. Infrared spectra were obtained with samples prepared as KBr pellets in the 400–4000 cm^{−1} region with a Nicolet Impact 410 FTIR spectrophotometer. Reflectance spectra were carried out with a Cary 2415 spectrometer in the range 200–2000 nm. For UV/Vis solution measurements, a Varian UV/Vis/NIR spectrophotometer was employed in the range 200–900 nm. X-band EPR spectra were recorded with a Bruker EMX spectrometer, equipped with a standard Oxford continuous-flow cryostat. Magnetic measurements of powdered samples were carried out in the temperature range 1.8–300 K using a Quantum Design MPMS-7 Squid magnetometer. Diamagnetic corrections were estimated from Pascal tables.

X-ray Crystallographic Studies: Data were collected at low temperature ($T = 160$ K) with an IPDS STOE diffractometer for **1** and an XCALIBUR-CCD OXFORD DIFFRACTION diffractometer for **2**, both equipped with a Nitrogen Cooler Device, an Enraf-Nonius CAD4 was used for **3**. Graphite-monochromated Mo- K_α radiation ($\lambda = 0.71073$ Å) was employed in all cases. Semi-empirical absorption corrections: DIFABS^[43] were applied on **1** and **2**, and a ϕ -scan method^[44] on **3**. Structures were solved by Direct Methods using SIR92^[45] (**1**, **2**) and (SHELXS-97)^[46] (**3**), and refined by least-squares procedures on F^2 with the aid of SHELXL-97,^[47] included in the package WinGX.^[48] The Atomic Scattering Factors were taken from the International Tables for X-ray Crystallography.^[49] All hydrogen atoms were located on difference Fourier maps, and refined by using a riding model with a common isotropic thermal parameter, except the H(1n), H(2n) hydrogen atoms connected to nitrogen atoms N(4) in **1** and **2**, which were isotropically refined. For the three compounds all non-hydrogen atoms were anisotropically refined. Drawings were performed by using the programs CAMERON^[50] and ORTEP32^[51] with 50% probability displacement ellipsoids for non-hydrogen atoms. CCDC-187690, -187691 and -187508 for compounds **1**, **2** and **3**, respectively, contain the supplementary crystallographic data for this paper. These data can be obtained free of charge from the Cambridge Crystallographic Data Centre, 12 Union Road, Cambridge CB2 1EZ, UK; Fax: (internat.) + 44-1223/336-033; E-mail: deposit@ccdc.cam.ac.uk.

Acknowledgments

We thank Dr. J. J. Delgado (SCAI, Universidad de Burgos, Spain) for the elemental analyses and Prof. R. Olazcuaga and Dr. F. Guillen (CNRS, Pessac, France) for the reflectance measurements. This work has been carried out with the financial support of the Basque Government (PI99/53). P. G.-S. thanks to the Universidad de Burgos for a Doctoral Fellowship.

- [1] [1a] M. J. M. Campbell, *Coord. Chem. Rev.* **1975**, *15*, 279–319. [1b] S. Padhyé, G. B. Kauffman, *Coord. Chem. Rev.* **1985**, *63*, 127–160. [1c] D. X. West, S. B. Padhyé, P. B. Sonawane, *Struct. Bonding* **1991**, *76*, 1–50. [1d] D. X. West, A. E. Liberta, S. B. Padhyé, R. C. Chikate, P. B. Sonawane, A. S. Kumbhar, R. G. Yerande, *Coord. Chem. Rev.* **1993**, *123*, 49–71.
- [2] J. García-Tojal, M. K. Urriaga, R. Cortés, L. Lezama, T. Rojo, M. I. Arriortua, *J. Chem. Soc., Dalton Trans.* **1994**, 2233–2238.
- [3] J. García-Tojal, L. Lezama, J. L. Pizarro, M. Insausti, M. I. Arriortua, T. Rojo, *Polyhedron* **1999**, *18*, 3703–3711.
- [4] C. F. Bell, C. R. Theocharis, *Acta Crystallogr., Sect. C* **1987**, *43*, 26–29.
- [5] A. G. Bingham, H. Böge, A. Müller, E. W. Ainscough, A. M. Brodie, *J. Chem. Soc., Dalton Trans.* **1987**, 493–499.
- [6] J. García-Tojal, T. Rojo, *Polyhedron* **1999**, *18*, 1123–1130, and references therein.
- [7] F. E. Anderson, C. J. Duca, J. V. Scudi, *J. Am. Chem. Soc.* **1951**, *73*, 4967–4968.
- [8] C. F. Bell, K. A. K. Lott, N. Hearn, *Polyhedron* **1987**, *6*, 39–44.
- [9] A. W. Addison, T. N. Rao, J. Reedijk, J. van Rijn, G. C. Verschoor, *J. Chem. Soc., Dalton Trans.* **1984**, 1349–1356.
- [10] C. Janiak, *J. Chem. Soc., Dalton Trans.* **2000**, 3885–3896.
- [11] A. Albert, F. H. Cano, *Cristalografía*, Publicaciones CSIC, Madrid, **1995**.
- [12] I. Unamuno, J. M. Gutiérrez-Zorrilla, A. Luque, P. Román, L. Lezama, R. Calvo, T. Rojo, *Inorg. Chem.* **1998**, *37*, 6452–6460.
- [13] C. A. Hunter, J. K. M. Sanders, *J. Am. Chem. Soc.* **1990**, *112*, 5525–5534.
- [14] F. Cozzi, M. Cinquini, R. Annunziata, J. S. Siegel, *J. Am. Chem. Soc.* **1993**, *115*, 5330–5331.
- [15] C.-Y. Duan, B.-M. Wu, T. C. W. Mak, *J. Chem. Soc., Dalton Trans.* **1996**, 3485–3490.
- [16] Z.-H. Liu, C.-Y. Duan, J. Hu, X.-Z. You, *Inorg. Chem.* **1999**, *38*, 1719–1724.
- [17] H. Cheng, D. Chun-ying, F. Chen-jie, L. Yong-jiang, M. Qun-jin, *J. Chem. Soc., Dalton Trans.* **2000**, 1207–1212.
- [18] L. Ze-hua, D. Chun-ying, L. Ji-hui, L. Yong-jiang, M. Yu-hua, Y. Xiao-zeng You, *New. J. Chem.* **2000**, *24*, 1057–1062.
- [19] V. N. Byushkin, Y. M. Chumakov, N. M. Samus, I. O. Baka, *Zh. Strukt. Khim.* **1987**, *28*, 140–142.
- [20] M. K. Urriaga, M. I. Arriortua, J. García-Tojal, T. Rojo, *Acta Crystallogr., Sect. C* **1995**, *51*, 2172–2174.
- [21] Z. Lu, C. White, A. L. Rheingold, R. H. Crabtree, *Inorg. Chem.* **1993**, *32*, 3991–3994.
- [22] G. W. Bushnell, A. Y. M. Tsang, *Can. J. Chem.* **1979**, *57*, 603–607.
- [23] M. R. Taylor, J. P. Glusker, E. J. Gabe, J. A. Minkin, *Bioinorg. Chem.* **1974**, *3*, 189.
- [24] L. E. Warren, W. E. Hatfield, *Chem. Phys. Lett.* **1970**, *7*, 371.
- [25] G. A. Kiosse, V. K. Rotaru, A. V. Ablov, T. I. Malinovskii, N. I. Belichuk, *Russ. J. Inorg. Chem.* **1973**, *18*, 757–758.
- [26] E. W. Ainscough, A. M. Brodie, J. D. Ranford, J. M. Waters, K. S. Murray, *Inorg. Chim. Acta* **1992**, *197*, 107–115.
- [27] B. Moubarak, K. S. Murray, J. D. Ranford, X. Wang, Y. Xu, *Chem. Commun.* **1998**, 353–354.
- [28] [28a] M.-B. Ferrari, G. G. Fava, C. Pelizzi, P. Tarasconi, G. Tosi, *J. Chem. Soc., Dalton Trans.* **1987**, 227–233. [28b] D. Kovala-Demertzi, N. Kourkouvelis, D. X. West, J. Valdés-Martínez, S. Hernández-Ortega, *Eur. J. Inorg. Chem.* **1998**, 861–863. [28c] D. Kovala-Demertzi, N. Kourkouvelis, M. A. Demertzis, J. R. Miller, C. S. Frampton, J. K. Swearingen, D. X. West, *Eur. J. Inorg. Chem.* **2000**, 727–734.
- [29] M. C. Jain, R. K. Sharma, P. C. Jain, *J. Inorg. Nucl. Chem.* **1980**, *42*, 1229.
- [30] G. B. Deacon, R. J. Phillips, *Coord. Chem. Rev.* **1980**, *33*, 227.
- [31] K. Nakamoto, *Infrared and Raman Spectra of Inorganic and Coordination Compounds*, 5th ed., Wiley, New York, **1997**, pp. 50, 60.
- [32] E. S. Stern, C. J. Timmons, *Electronic Absorption Spectroscopy in Organic Chemistry*, Edward Arnold, London, **1970**.
- [33] D. X. West, M. A. Lockwood, J. N. Albert, A. E. Liberta, *Spectrochim. Acta* **1991**, *49A*, 1809–1816.
- [34] D. X. West, Y. Yang, T. L. Klein, K. I. Goldberg, A. E. Liberta, J. Valdés-Martínez, R. A. Toscano, *Polyhedron* **1995**, *14*, 1681–1693.
- [35] W. E. Antholine, J. M. Knight, D. H. Petering, *Inorg. Chem.* **1977**, *16*, 569–574.
- [36] H. Beraldo, L. Tosi, *Inorg. Chim. Acta* **1986**, *125*, 173–182.
- [37] B. Bleaney, K. D. Bowers, *Proc. R. Soc. London, Ser. A* **1952**, *214*, 451.
- [38] P. J. Hay, J. C. Thibeault, R. Hoffmann, *J. Am. Chem. Soc.* **1975**, *97*, 4884–4899.
- [39] CACAO Program, Computer Aided Composition of Atomic Orbitals, PC version 4.0, July **1994**: C. Mealli, D. M. Proserpio, *J. Chem. Educ.* **1990**, *67*, 399–402.
- [40] J. García-Tojal, J. L. Pizarro, L. Lezama, M. I. Arriortua, T. Rojo, *Inorg. Chim. Acta* **1998**, *278*, 150–158.
- [41] P. Román, C. Guzmán-Miralles, A. Luque, J. I. Beitia, J. Cano, F. Lloret, M. Julve, S. Alvarez, *Inorg. Chem.* **1996**, *35*, 3741–3751.
- [42] J. Cano, P. Alemany, S. Alvarez, M. Verdaguier, E. Ruiz, *Chem. Eur. J.* **1998**, *4*, 476–484.
- [43] N. Walker, D. Stuart, *Acta Crystallogr., Sect. A* **1983**, *39*, 158–166.
- [44] A. C. T. North, D. C. Phillips, F. S. Mathews, *Acta Crystallogr., Sect. A* **1968**, *24*, 351.
- [45] A. Altomare, G. Casciarano, C. Giacovazzo, A. Guagliardi, *J. Appl. Crystallogr.* **1993**, *26*, 343–350.
- [46] G. M. Sheldrick, *SHELXS-97, A Program for Crystal Structure Solution*, Univ. of Göttingen, Göttingen, Germany, **1997**.

- [47] G. M. Sheldrick, *SHELX97, Programs for Crystal Structure Analysis (Release 97-2)*, Institut für Anorganische Chemie der Universität, Tammanstrasse 4, D-3400 Göttingen, Germany, **1998**.
- [48] *WINGX – 1. 63, Integrated System of Windows Programs for the Solution, Refinement and Analysis of Single Crystal X-ray Diffraction Data*: L. Farrugia, *J. Appl. Crystallogr.* **1999**, *32*, 837–838.
- [49] *International Tables for X-ray Crystallography*, Kynoch Press, Birmingham, England, **1974**, vol. IV.
- [50] D. M. Watkin, L. Pearce, C. K. Prout, *CAMERON, A Molecular Graphics Package*, Chemical Crystallography Laboratory, University of Oxford, England, **1993**.
- [51] L. J. Farrugia, *J. Appl. Crystallogr.* **1997**, *30*, 565.

Received June 14, 2002
[I02316]